

# Bitongqing Attenuates CIA Rats by Suppressing Macrophage Pyroptosis and Modulating the NLRP3/Caspase-1/GSDMD Pathway

Yunxia Wu<sup>1,\*</sup>, Yue Zhang<sup>1,\*</sup>, Zishan Wang<sup>1</sup>, Yun Lu<sup>1</sup>, Yabei Wang<sup>1</sup>, Jie Pan<sup>1</sup>, Chenxi Liu<sup>1</sup>, Wen Zhu<sup>2,\*</sup>, Yue Wang<sup>2,\*</sup>

<sup>1</sup>Academy of First Clinical Medicine, Nanjing University of Chinese Medicine, Nanjing, Jiangsu, People's Republic of China; <sup>2</sup>Department of Rheumatology & Immunology, Affiliated Hospital of Nanjing University of Chinese Medicine, Nanjing, Jiangsu, People's Republic of China

\*These authors contributed equally to this work

Correspondence: Yue Wang; Wen Zhu, Department of Rheumatology & Immunology, Affiliated Hospital of Nanjing University of Chinese Medicine, Nanjing, Jiangsu, People's Republic of China, Email wangyue@njucm.edu.cn; zhuwen@njucm.edu.cn

**Background:** Rheumatoid arthritis (RA) is an autoimmune disease characterized by synovitis and inflammatory cell infiltration. The traditional Chinese medicine prescription, Bitongqing (BTQ) exhibited significant efficacy in the clinical treatment of RA. However, the potential therapeutic mechanisms of BTQ in treating RA have not been fully investigated. This study aims to elucidate the effect of BTQ on collagen-induced arthritis (CIA) rat macrophage pyroptosis, providing a theoretical basis for treating RA.

**Methods:** This research employed liquid chromatography-mass spectrometry (LC-MS) to identify the primary components of BTQ. The therapeutic effects of BTQ were evaluated in a rat model of CIA. In vivo experiments were conducted using pathohistological staining, immunofluorescence, micro-CT, and Western blotting. Next, Mouse leukemia cells of monocyte macrophage cells (RAW264.7) were induced to undergo pyroptosis using lipopolysaccharide (LPS) and adenosine triphosphate (ATP), and the impact of BTQ on RAW264.7 macrophages was assessed through cell viability, immunofluorescence analysis, lactate dehydrogenase (LDH) secretion measurement, and Western blotting.

**Results:** BTQ had a therapeutic effect on CIA rats, which was mainly manifested as a reduction in joint inflammation, foot swelling, bone erosion, and amelioration of pathological changes in these rats. Further studies revealed that BTQ inhibited the levels of cytokine production interleukin-18 (IL-18) and interleukin-1 $\beta$  (IL-1 $\beta$ ), and likewise, it inhibited the expression of key proteins in the NOD-like receptor thermal protein domain associated protein 3 (NLRP3) mediated pyroptosis in the synovial tissues of CIA rats. The results of in vitro experiments demonstrated that BTQ attenuated LDH secretion, decreased IL-18 and IL-1 $\beta$  cytokine production, and down-regulated expression of key proteins involved in the NLRP3-mediated pyroptosis on RAW264.7 macrophages.

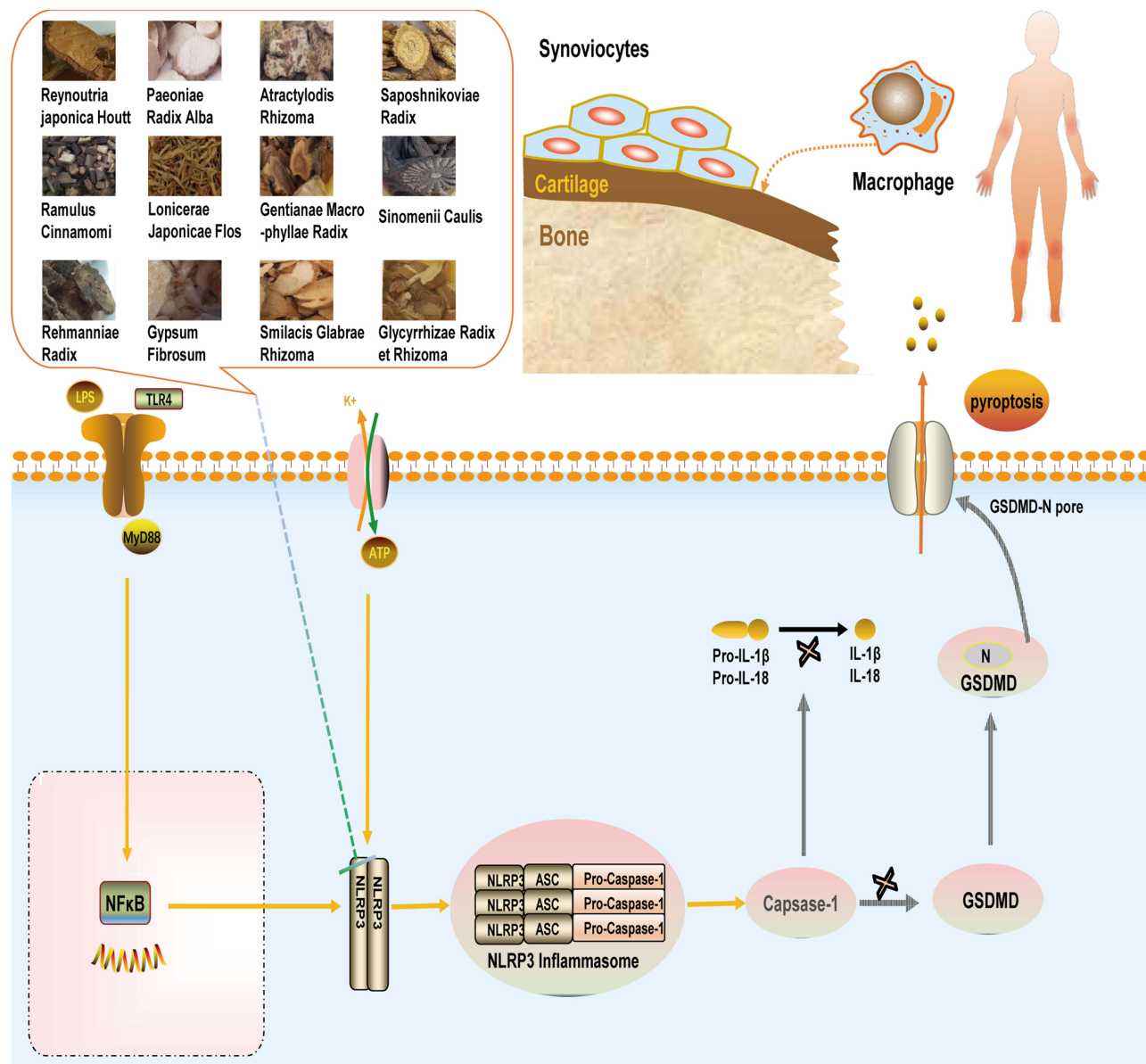
**Conclusion:** The therapeutic potential of BTQ in CIA lies in its ability to inhibit NLRP3-mediated macrophage pyroptosis, thereby suggesting a promising strategy for the treatment of RA.

**Keywords:** rheumatoid arthritis, Bitongqing, pyroptosis, NLRP3 inflammasome, macrophage

## Introduction

Rheumatoid arthritis (RA) is a persistent and systemic autoimmune disease characterized by synovial inflammation, destruction of bone and cartilage, and invasion of inflammatory cells.<sup>1</sup> It affects approximately 0.5–1.0% of the global adult population annually and is associated with joint discomfort, cartilage abnormalities, reduced flexibility, and joint space narrowing, thereby imposing a significant societal burden.<sup>2,3</sup> Currently, disease-modifying anti-rheumatic drugs (DMARDs), nonsteroidal anti-inflammatory drugs (NSAIDs), glucocorticoids, and biological agents are the most commonly prescribed medications for RA,<sup>4</sup> aiming to alleviate synovitis and systemic inflammation while improving joint function. However, these conventional therapies face challenges related to suboptimal patient care,<sup>5</sup> infection risks,<sup>6</sup> and high costs.<sup>7</sup> Therefore, it is imperative to explore alternative treatment options for rheumatoid arthritis.

## Graphical Abstract



Research findings have indicated a correlation between the excessive activation of immune and nonimmune cells and the development of RA.<sup>8</sup> Macrophages, which are highly expressed during RA-related inflammation, play pivotal roles in perpetuating inflammation and tissue damage in RA patients.<sup>9,10</sup> Moreover, an abundance of infiltrating macrophages within the synovium is considered an early indicator of RA.<sup>11</sup> Consequently, the extent of macrophage infiltration correlates with joint erosion severity and highlights the therapeutic potential of depleting activated macrophages from inflamed tissues.<sup>10</sup> Recent studies have revealed a strong association between pyroptosis and RA onset,<sup>12–14</sup> which represents a type of cellular demise initiated by the activation of the nucleotide-binding oligomerization domain-like receptor protein 3 (NLRP3) inflammasome, and marked by cell enlargement, membrane rupture, and the ensuing emission of inflammatory cytokines and warning signals.<sup>15</sup> This mechanism stimulates cytokine secretion and activates macrophages as well as T- lymphocytes, thereby initiating robust inflammatory reactions and immune phagocytosis.<sup>16,17</sup>

The inhibition of NLRP3 inflammasome-mediated macrophage pyroptosis has been reported to effectively alleviate various inflammatory diseases including RA, gout, type 2 diabetes mellitus (T2DM), and atherosclerosis among others.<sup>18–22</sup>

Traditional Chinese medicine (TCM) is an attractive option for the treatment of clinically active RA.<sup>23</sup> Compared with synthetic medications, they are more accessible, safer, and more cost effective.<sup>7</sup> Bitongqing (BTQ) is a TCM prescription. It contains Guizhi (*Neolitsea cactia* (L.) *Kosterm.*), Baishao (*Paeonia altaica*), Huzhang (*Reynoutria japonica* Houtt), Cangzhu (*Atractylodes lancea*), Fangfeng (*Saposhnikovia divaricate*), Jinyinhua (*Lonicera japonica* Thunb), Qinjiao (*Gentiana macrophylla* Pall), Qingfengteng (*Sinomenium acutum* (Thunb.) *Rehder*), Shengdi (*Rehmannia glutinosa* (Gaertn.) *DC.*), Shigao (*Gypsum Fibrosum*), Tufuling (*Smilax glabra* Roxb.), Gancao (*Glycyrrhiza uralensis* Fisch. *ex DC.*). BTQ was modified from Qinjiao Dihuang Tongbi Decoction (QDTD), which has been used for many years for the treatment of RA and has notable clinical effectiveness.<sup>24</sup> It has the potential to heat-clear, dehumidify, eliminate blood stasis and detoxification, markedly lower the serum concentrations of inflammatory factors, slow the progression of the disease, and relieve symptoms in RA patients.<sup>25</sup> Furthermore, a patent was granted by the China National Intellectual Property Administration (CNIPA) (Patent No. 108524740A). It is well known that BTQ is an alteration of Baihu-Guizhi decoction (BHGZD). The study has evidenced that Baihu-Guizhi decoction (BHGZD) may interact with TLR4/PI3K/AKT/NFκB signaling to inhibit NLRP3 inflammasome activation and modulate pyroptosis against active RA.<sup>26</sup> However, limited evidence exists regarding the involvement of BTQ in inhibiting NLRP3 inflammasome activation in RA. Therefore, further investigation is necessary to determine whether this process is linked to the inhibition of macrophage pyroptosis.

This research initially identified the key elements of BTQ using Liquid Chromatograph- Mass Spectrometer (LS-MS) methods, subsequently created a collagen-induced arthritis (CIA) rat model, and revealed the ability of BTQ to reduce arthritis symptoms in CIA rats through observation of overall conditions. Following a sequence of pharmacological experiments, the mechanism through which BTQ works to block the NLRP3/Caspase-1/GSDMD signaling pathway for RA therapy was established. The lipopolysaccharide (LPS) plus adenosine triphosphate (ATP)-induced RAW264.7 macrophage pyroptosis model was ultimately utilized to validate previous experimental findings.

## Materials and Methods

### Materials and Reagents

*Tripterysium Glycosides* (TG) (10 mg×50 tablets) were purchased from Zhejiang Deen Pharmaceutical Co., Ltd. We purchased methanol, ethanol, formic acid, and acetonitrile from Millipore (Massachusetts, USA) and ensured that all the chemicals and solvents met the criteria for analytical reagent or chromatographic quality.

### Preparation of the Bitongqing Decoction

The BTQ consists of 12 traditional Chinese medicines. The specific dosage is as follows: 15 g Guizhi (*Neolitsea cactia* (L.) *Kosterm.*), 15 g Baishao (*Paeonia altaica*), 15 g Huzhang (*Reynoutria japonica* Houtt), 15 g Cangzhu (*Atractylodes lancea*), 15 g Fangfeng (*Saposhnikovia divaricata*), 15 g Jinyinhua (*Lonicera japonica* Thunb), 15 g Qinjiao (*Gentiana macrophylla* Pall), 15 g Qingfengteng (*Sinomenium acutum* (Thunb.) *Rehder*), 30 g Shengdi (*Rehmannia glutinosa* (Gaertn.) *DC.*), 30 g Shigao (*Gypsum Fibrosum*), 30 g Tufuling (*Smilax glabra* Roxb.), 5 g Gancao (*Glycyrrhiza uralensis* Fisch. *ex DC.*). All herbal medicines use for BTQ were purchased from the Jiangsu Provincial Hospital of Traditional Chinese Medicine (Jiangsu, China). The quality of the drugs is controllable. The names of the plants were verified with <http://mpns.kew.org>. The samples were boiled evenly. *Gypsum Fibrosum* was added to boiling purified water, after which the mixture was boiled for 30 minutes. The remaining herbs were soaked in purified water for 30 minutes. Then herbal mixture was subsequently added to purified water supplemented with *Gypsum Fibrosum* after which the mixture was boiled at a high heat. The mixture was boiled quickly and then heated at a low temperature for 40 minutes. The decoction was repeated twice. The two decoctions were mixed and concentrated to a 1:1 solution (equivalent to 8.37 g of crude drug per milliliter of solution). The solution was stored at –20°C for future use.

## Preparation of Serum from Bitongqing

Following a week-long acclimation feeding period, 20 female SD rats received a BTQ solution of 19.35 g/kg/d, via gavage twice a day over a span of 7 days. Blood was drawn from the abdominal aorta following the final 12-hour gavage. After serum centrifugation, the mixture was deactivated at 56°C for half an hour and subsequently preserved at -80°C for future reference.

## LC-MS Analysis

### Metabolite Extraction

The specimen was vortexed with 80% methanol, subjected to sonication in an ice bath for 20 minutes, maintained at -20°C for 2 hours, and spun at  $16000 \times g$  for 20 minutes at 4°C, followed by evaporation of the supernatant in a high-speed vacuum centrifuge. To detect mass spectrometry, 50% methanol was added for re-solubilization, the mixture was centrifuged at  $20000 \times g$  for 15 minutes at 4°C, and the supernatant was subsequently extracted. After extraction, the liquid was collected through a 0.22  $\mu$ m filter and 6.0  $\mu$ L was sampled for analysis in the LC-MS system. The liquid chromatography-mass spectrometry conditions are detailed in [Supplementary Table 1](#) and [Supplementary Table 2](#).

### Data Preprocessing

The initial data were subjected to peak alignment, retention time adjustment, and identification of peak regions utilizing MSDIAL software. The process of identifying metabolite compositions involved precise matching of mass numbers (with a mass tolerance less than 10 ppm) and matching of secondary spectra (with a mass tolerance less than 0.01 Da).

## Animals and Grouping

Female SD rats ( $n=60$ , 6–8 weeks,  $200 \pm 20$  g in weight) were purchased from Hangzhou Medical College (Production License No. SCXK 2019-0002, Zhejiang, China). All animal experiments complied with the US Public Health Service Policy on the Use of Laboratory Animals.<sup>27</sup> All of the rats were kept in an environment free of specific pathogens (12 h light/dark cycle and  $24 \pm 2^\circ\text{C}$ ). Every experiment involving animals adhered to the established protocols and received approval from the Ethics Committee of Nanjing University of Chinese Medicine. Sixty rats in experiment were randomly divided into six groups (Control, CIA, BTQ-H, BTQ-M, BTQ-L, and TG,  $n = 10$ ).

## Collagen-Induced Arthritis (CIA) Induction and Treatment

The creation of the CIA rat model followed an earlier established methodology.<sup>28</sup> A mixture of equal amounts of bovine type II collagen (20022, Chondrex, USA) and complete Freund's adjuvant (F5881, Sigma-Aldrich, USA) (1:1, v/v) was prepared, and an initial immunization was achieved by subcutaneous injection of 0.2 mL of the mixture into the tail root of all the rats except the control rats. After day 7 of initial immunization, a second immunization was achieved by subcutaneous injection of 0.1 mL of bovine type II collagen mixed with incomplete Freund's adjuvant (F5506; Sigma-Aldrich, USA) into the tail root of all the rats except the control rats. Beginning on the 22nd day, the drug was administered by gavage once a day, and the plants in each group were treated as follows: control group (with saline), CIA group (with saline), BTQ-L group (with low-dose BTQ: 9.68 g/kg/d), BTQ-M group (with medium-dose BTQ: 19.35 g/kg/d), BTQ-H group (with high-dose BTQ: 38.7 g/kg/d), and TG group (with tretinoin tablet suspension: 9.45 mg/kg/d). On day 49 (in accordance with the guidelines of the Animal Care and Ethics Committee of the Animal Centre of Nanjing University of Traditional Chinese Medicine), all the rats were killed, and specimens were collected.

## Assessment of Arthritis Severity

Arthritis severity was independently evaluated every 7 days by three researchers unaware of the sequence in which the rats emerged. The observations adhered to the methodology set forth in the preceding research.<sup>29</sup> In brief, the paws of the rats were analyzed and rated on a 0–8 scale (0–4 for each paw, summing up the two paws' scores): 0, normal; 1, mild joint swelling; 2, localized, notable joint swelling; 3, significant joint swelling with restricted mobility; and 4, widespread joint swelling without joint bending capability.<sup>30</sup>



## Thymus and Spleen Indices

Immediately after sacrifice on the 49th day of the experiment, the thymus and the spleen were removed and weighed. The index for the thymus or spleen was calculated by dividing the weight of these organs by the body weight (mg/g).

## Histopathological Observations

Ankle bone tissues were fixed in 4% paraformaldehyde and then dehydrated through a graded series of alcohols. Subsequently, the samples were embedded in paraffin, and the sections were stained with H&E and Safranin O fast green dye. Light microscopy was used to analyze bone and synovial tissues to evaluate the destruction of cartilage and inflammation in the synovial area, respectively.

## Micro-CT

Radiographic imaging was used to observe bone damage. The rats were subjected to a microcomputed tomography (CT) scan of their toe and knee joints. A Quantum GX micro-CT scanner (PerkinElmer, Inc, Waltham, MA) was used for the procedure.

## Cell Culture, Induction, and Treatment

A mouse macrophage line (Raw264.7 cells, SenBeiJia Biological Technology Co., Ltd., Nanjing, China) was used for in vitro experimental validation. Raw264.7 macrophages were maintained in DMEM (G4511, Servicebio, Wuhan, China) at 37°C in a 5% CO<sub>2</sub> atmosphere supplemented with 10% fetal bovine serum (FBS, 10270–106, Gibco, USA) and a 1% penicillin-streptomycin mixture (C0222, Beyotime, Shanghai, China) to validate the use of low-passage Raw264.7 macrophages.

RAW264.7 macrophages were induced with 1 µg/mL lipopolysaccharide (LPS, Escherichia coli (O111: B4), L4391, Sigma-Aldrich, St. Louis, USA) for 24 hours, followed by 5 mM adenosine triphosphate (ATP, HY-B2176, MCE, New Jersey, USA) for 1 hour and kept at 37°C in a 5% CO<sub>2</sub> incubator.

A cell counting kit-8 (CCK-8) test was conducted 24 hours after treatment with various concentrations of BTQ-containing serum to evaluate cell growth following the manufacturer's instructions (BS350B, Biosharp, Shanghai, China).

## Enzyme-Linked Immunosorbent Assay

On day 50, all rats were anesthetized and positioned on their backs. Blood samples were taken from the abdominal aorta via a single-use negative pressure anticoagulation tube. The blood was kept at ambient temperature for 30 minutes and then centrifuged at 3000 rpm for 15 minutes at 4°C, after which the transparent liquid above the sediment was collected. At the end of cell culture, the supernatant was gathered through centrifugation, and the levels of IL-1β and IL-18 in the cells and rat serum were measured using ELISA kits (ZCIBIO, Shanghai, China) according to the manufacturer's instructions.

## Lactic Dehydrogenase Assay

RAW264.7 cells were seeded in 96-well plates, subjected to the appropriate treatment and centrifuged at 400 × g for five minutes. Afterwards, 120 µL of the extracted supernatant was transferred to a fresh 96-well plate, and 60 µL of LDH detection liquid was added. Finally, the plate was incubated at ambient temperature for half an hour, after which the absorbance was measured at 490 nm using an enzyme label analyzer (Rayto RT-6100, USA); specific procedures were performed with LDH release assay kit (C0017, Beyotime, Shanghai, China).

## Immunofluorescence Staining

The cells or synovial tissue were fixed in 4% paraformaldehyde and subsequently encased in paraffin. Subsequently, the paraffin was treated with an eco-friendly deparaffinizing agent (G1128, Servicebio, Wuhan, China) for deparaffinization and then washed with anhydrous ethanol and distilled water. The sections were blocked for 1 h by incubation with 3% bovine serum albumin (BSA). The sections were then incubated overnight at 4°C with primary antibody against GSDMD (GB114198, Servicebio, Wuhan, China), followed by incubation with secondary antibody conjugated to the primary

antibody for 50 minutes at room temperature without illumination. Finally, the nuclei were stained with DAPI (G1012, Servicebio, Wuhan, China) for 10 minutes, and the sections were sealed with an anti-fluorescent bursting explosive and stored at 4°C in the dark. Images were taken and visualized with an orthogonal fluorescence microscope (Nikon Eclipse C1, Japan).

## Hoechst 33342 and PI Fluorescence Staining

Cell death was evaluated using Hoechst 33342 (c1027, Servicebio, Wuhan, China) and PI (40755ES64, Yeasen, Shanghai, China) fluorescence staining. First, RAW264.7 cells were induced and treated. After removal of the supernatants, the cells were rinsed three times with PBS. Next, Hoechst 33342 was added to each well, and the cells were kept in darkness at 37°C for 10 minutes. PI was then added, and the mixture was incubated for 20 minutes at ambient temperature in the dark. Finally, the stained cells were analyzed using an inverted fluorescence microscope (OLYMPUS IX71), followed by image capture and display.

## Western Blotting

Total protein derived from synovial tissue and RAW 264.7 cells was subjected to ultrasonic lysis in RIPA buffer. The concentration of protein was determined using the BCA method (20201-A, YEASEN, Shanghai, China), and proteins were separated via standard 10% SDS-PAGE and transferred to a polyvinylidene difluoride membrane (PVDF Millipore, USA). Subsequently, the membranes were blocked using protein blocking buffer (P30500, NCM Biotech, China) for an hour at ambient temperature, followed by an overnight incubation with the primary antibody at 4°C. The sections were then rinsed with TBS-Tween and incubated with suitable secondary antibodies for an hour at ambient temperature. The blots were visualized with chemiluminescent agents (36208ES76, YEASEN, Shanghai, China), and gray level analysis was performed using ImageJ software. The primary antibodies used in the experiment were as follows: total and cleaved N-terminal GSDMD (P30823), NLRP3 (T55651), and Caspase-1 (M025280) were purchased from Abmart Shanghai Co., Ltd. The anti-ASC (YT0365) antibody was purchased from ImmunoWay (Texas, USA).

## Statistical Analyses

Statistical analysis was conducted using GraphPad Prism 8.0 software. The data are displayed as the mean  $\pm$  SD. Group comparisons were made by one-way analysis of variance (ANOVA), and Dunnett's multiple comparison test was used for three or more groups. Changes were considered to be statistically significant if the *p*-value was less than 0.05.

## Results

### LC-MS Detection and Base Peak Chromatography (BPC)

The spectrum of the BPC is derived by sequentially illustrating the strength of the most intense ion in the mass spectrogram at various intervals. [Figure 1A](#) and [B](#) shows the BPC of BTQ in the form of positive and negative ions, respectively. The main chemical constituents contained in BTQ are detailed in [Supplementary Table 3](#).

### BTQ Reduced the Severity of Arthritis in CIA Model Rats

For the purpose of determining the therapeutic effect of BTQ on rheumatoid arthritis, we successfully established a collagen-induced arthritis model simulating rheumatoid arthritis with the following special steps. ([Figure 2A](#)). After day 14 of initial immunization, CIA rats showed progressive redness and swelling of the foot, reaching their highest levels of arthritis and paw swelling on day 21 ([Figure 2B](#) and [C](#)). Different doses of BTQ and tretinoin tablets were given continuously by gavage for 4 weeks. After the third week of gavage, there was a notable decrease in arthritis scores and toe swelling in the treated group compared to the model group, and there was a significant increase in body weight from before administration ([Figure 2D](#)). Subsequently, we separately evaluated the thymus and spleen indices in the different subgroups, and found that these indices significantly decreased in response to BTQ treatment ([Figure 2E](#) and [F](#)). Additionally, histological analysis of ankle joint sections from normal rats revealed intact joint surfaces, consistent joint spaces, and an organized synovial cell layer on the outer surface of the cartilage. In contrast, CIA rats exhibited hyperproliferative and disorganized synovial cells

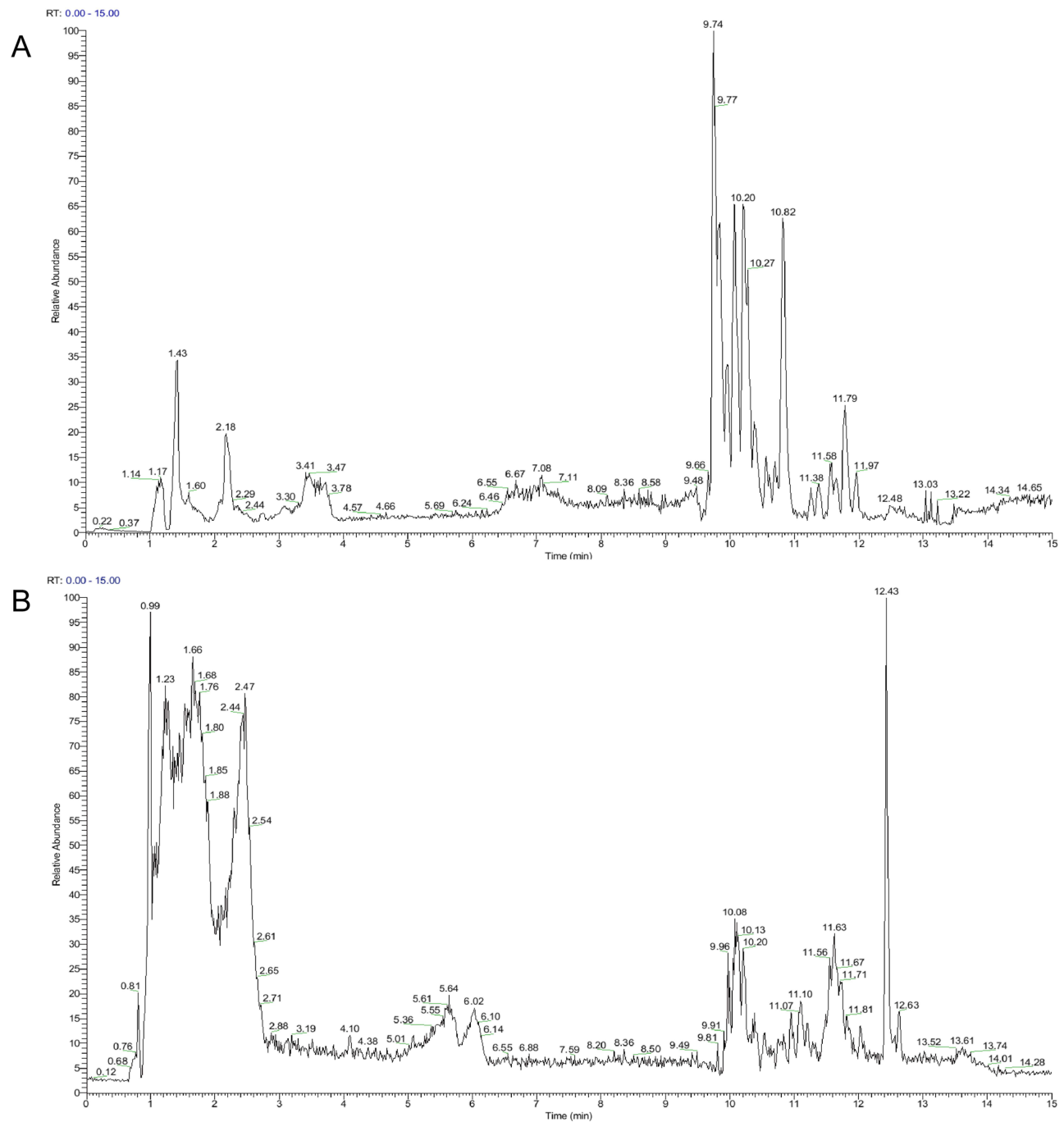


**Figure 1** BPC in positive and negative ion modes of BTQ. **(A)** BPC in positive ion mode for BTQ. **(B)** BPC in negative ion mode for BTQ.

within their joint tissues, accompanied by extensive infiltration of inflammatory cells and erosion of cartilage. Importantly, the administration of BTQ effectively ameliorated these pathological changes (Figure 2G). Micro-CT and three-dimensional reconstruction also revealed that BTQ effectively ameliorated bone destruction in CIA rats (Figure 3).

## BTQ Inhibits NLRP3 Inflammasome-Induced Pyroptosis in CIA Rats

GSDMD serves as a key marker for pyroptosis and regulates the secretion of proinflammatory cytokines.<sup>31</sup> Immunofluorescence staining for GSDMD revealed that GSDMD expression was greater in the CIA group than in the control group. In contrast to those in the CIA group, the BTQ and TG groups exhibited reduced GSDMD expression, and the BTQ

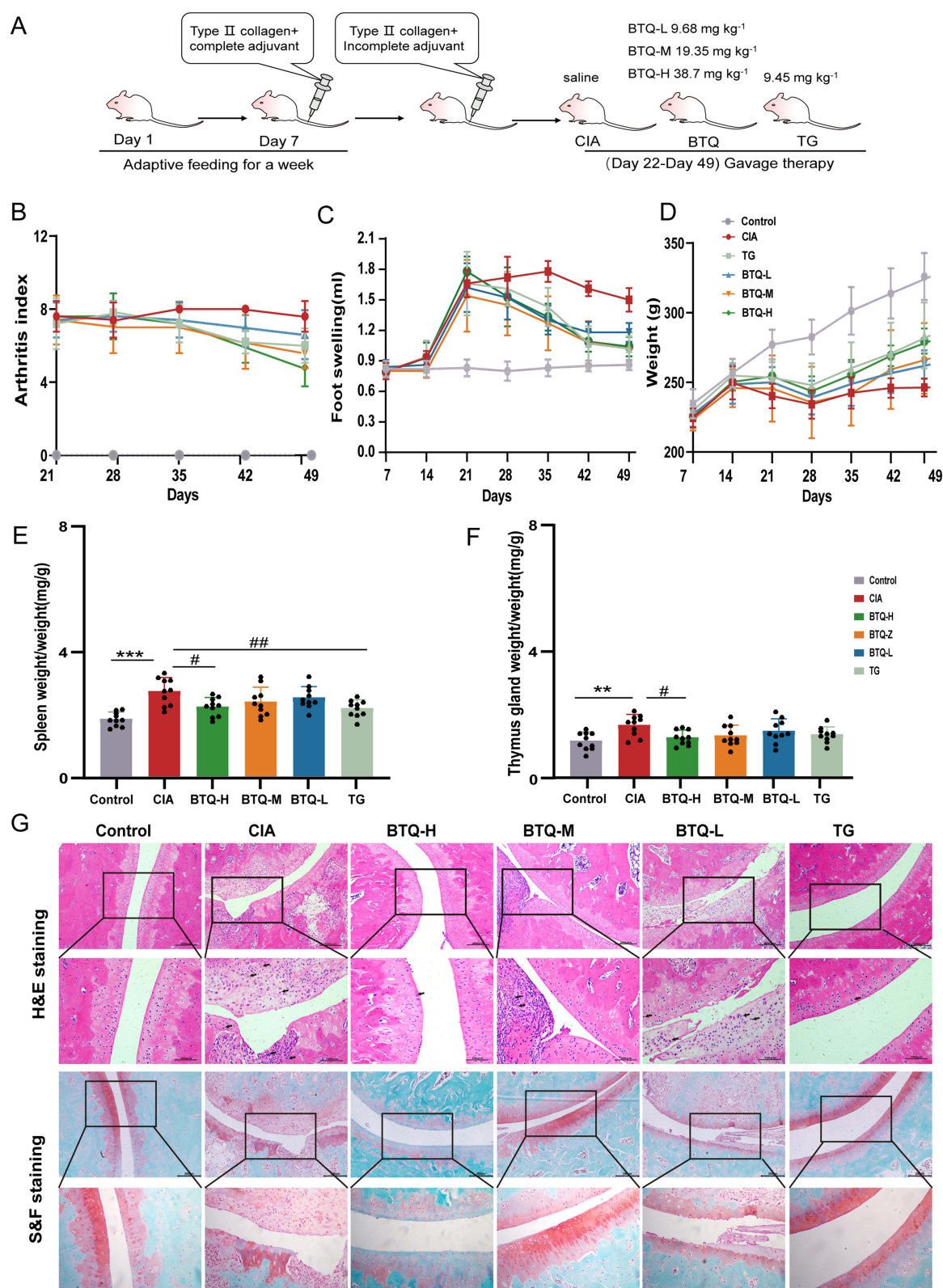


**Figure 2** The effect of BTQ on the severity of arthritis in different groups of CIA rats. **(A)** Diagram illustrating the design of the animal experiments. **(B)** The arthritis Index ( $n=10$ ), **(C)** incidence of foot swelling and **(D)** body weight were evaluated every 7 days until day 49 ( $n=10$ ). **(E)** Spleen indices ( $n=10$ ), **(F)** Thymus index ( $n=10$ ). **(G)** Variations in ankle joint pathology observed using hematoxylin and eosin (H&E) and safranin O fast green (S&F) in different groups (Scale bar=200 $\mu$ m, 100 $\mu$ m). \*\*and \*\*\*,  $p < 0.01$  and  $p < 0.001$ , respectively, compared with the normal control group; # and ##,  $p < 0.05$  and  $p < 0.01$ , respectively, compared with the CIA group ( $n=3$ ).



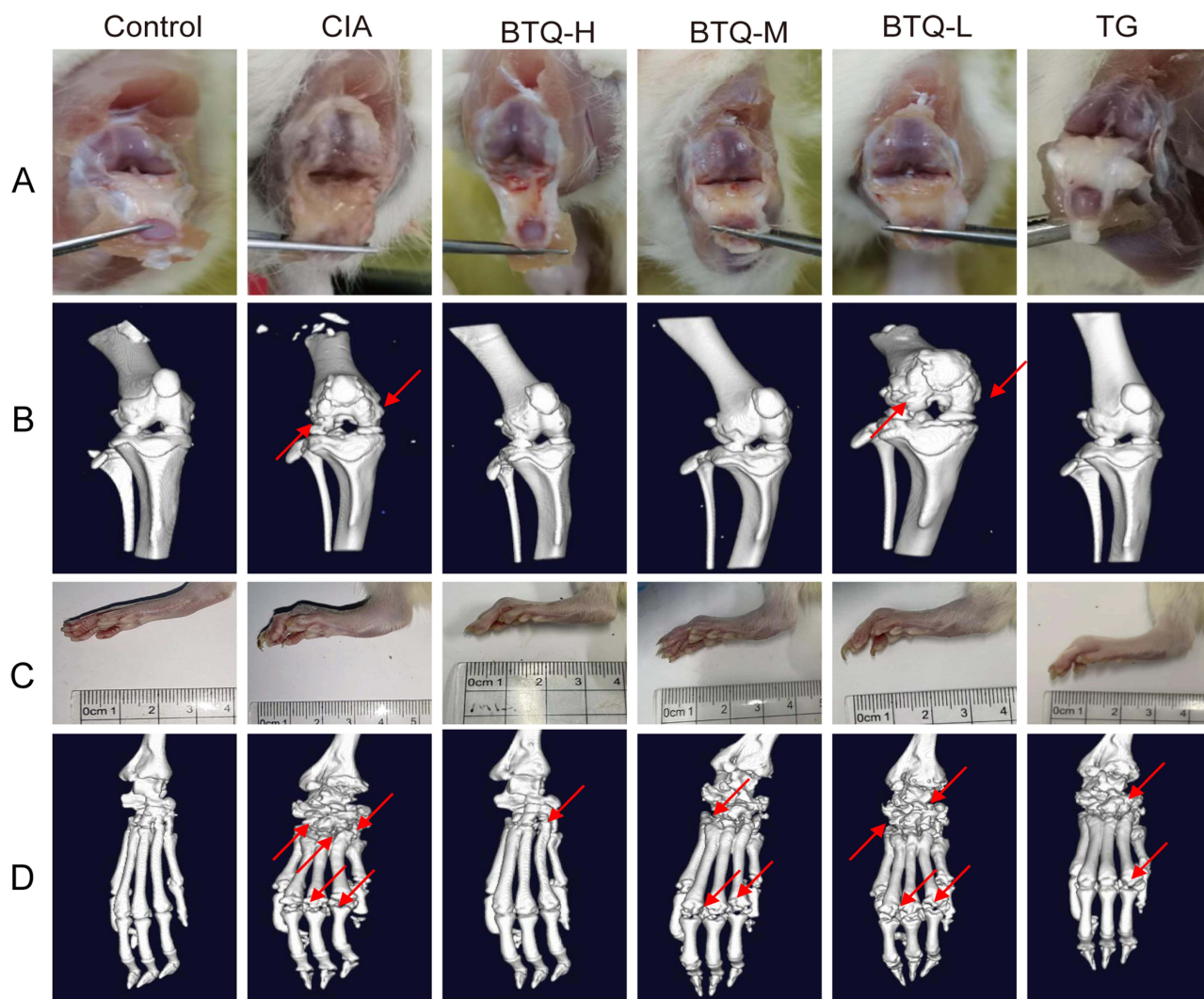


**Figure 3** BTQ treatment attenuates bone destruction in different groups of CIA rats (n=3). (A) and (B) are representative knee images and micro-CT scans from different CIA groups. (C) and (D) are representative ankle images and micro-computed tomography (micro-CT) scans from different CIA groups (Red arrows represents bone destruction).

group exhibited a dose-dependent inhibitory effect (Figure 4A). Notably, the accumulation of GSDMD and the formation of membrane pores cause the rupture of cell membranes, resulting in the secretion of IL-1 $\beta$  and IL-18, which is characteristic of pyroptosis.<sup>32</sup> Our ELISA analysis of inflammatory factor release in rat serum revealed higher IL-18 and IL-1 $\beta$  levels in the CIA group than in the control group, whereas the IL-18 and IL-1 $\beta$  levels in rats treated with BTQ and TG were notably lower than those in the CIA group (Figure 4B and C). To better understand the inhibitory effect of BTQ on pyroptosis, the presence of pyroptosis-associated proteins in rat synovial tissues was determined by Western blotting. The results indicated a notable increase in the expression of proteins linked to pyroptosis in the CIA group compared with the normal group, and both the BTQ and TG treatments resulted in a significant reduction in the expression of these proteins. These findings indicated that BTQ reduced the incidence of pyroptosis induced by GSDMD (Figure 5).

## Treatment with BTQ in Serum Suppresses LPS Plus ATP-Induced Cell Death in Raw264.7 Cells

Initially, the toxicity of BTQ in combination with drug-containing serum on Raw 264.7 macrophage proliferation was assessed using a CCK8 assay, which revealed no toxic effects at concentrations of 5, 10, or 15% as depicted in Figure 6A. Consequently, we chose serum containing 5, 10, or 15% BTQ for subsequent experimental treatments. Experiments revealed that varying concentrations of the drug decreased LDH secretion (Figure 6B), primarily to confirm cell membrane integrity and the discharge



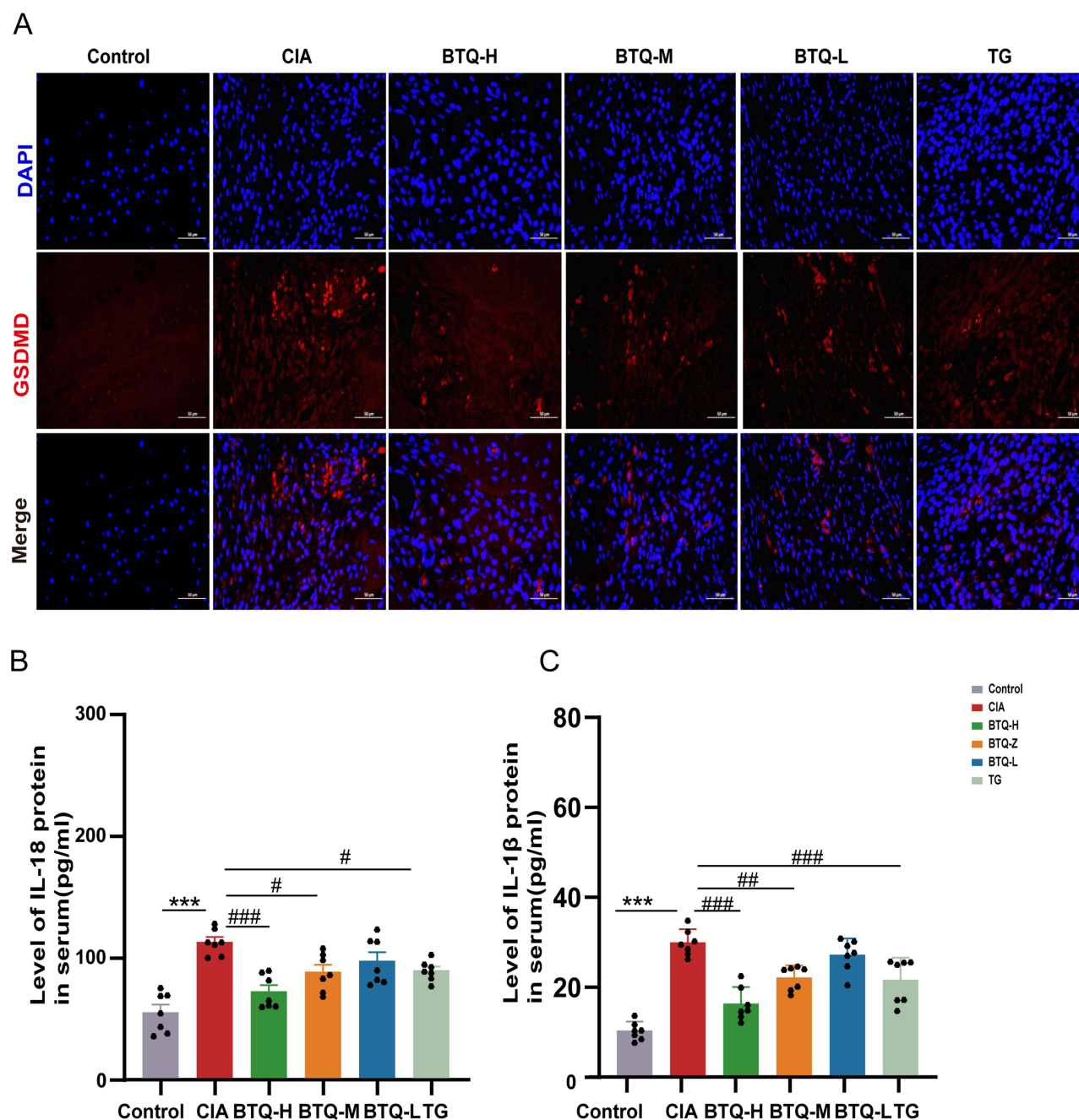


**Figure 4** Effect of BTQ on inflammation in CIA rats in different groups. **(A)** Expression of GSDMD protein in the ankle joints of CIA rats (GSDMD Cy3 red, DAPI blue, scale bar represents 50  $\mu$ m) detected by immunofluorescence staining. **(B and C)** The detection of secreted IL-1 $\beta$  and IL-18 in the serum of CIA rats was performed by ELISA ( $n=7$ ). \*\*\*,  $p < 0.001$ , compared with the normal control group; #, ##, and ###,  $p < 0.05$ ,  $p < 0.01$ , and  $p < 0.001$ , respectively, compared with the CIA group.

of cell contents. Subsequently, our analysis of IL-18 and IL-1 $\beta$  levels in cell culture supernatants using ELISA revealed that treatment with serum containing BTQ reduced the expression of the inflammatory factors IL-18 and IL-1 $\beta$  (Figure 6C and D). Ultimately, to further explore the extent of cell death, Hoechst 33342/PI immunofluorescence was used to detect a notable reduction in the number of PI-positive cells and a decrease in cell fatality (Figure 6E).

## Treatment with BTQ in Serum Inhibits NLRP3 Inflammasome-Induced Pyroptosis in Raw264.7 Cells

In an effort to further explore how BTQ-containing serum works in treating Raw264.7 cell pyroptosis, researchers have pinpointed proteins linked to pyroptosis through immunofluorescence staining and Western blotting analysis.

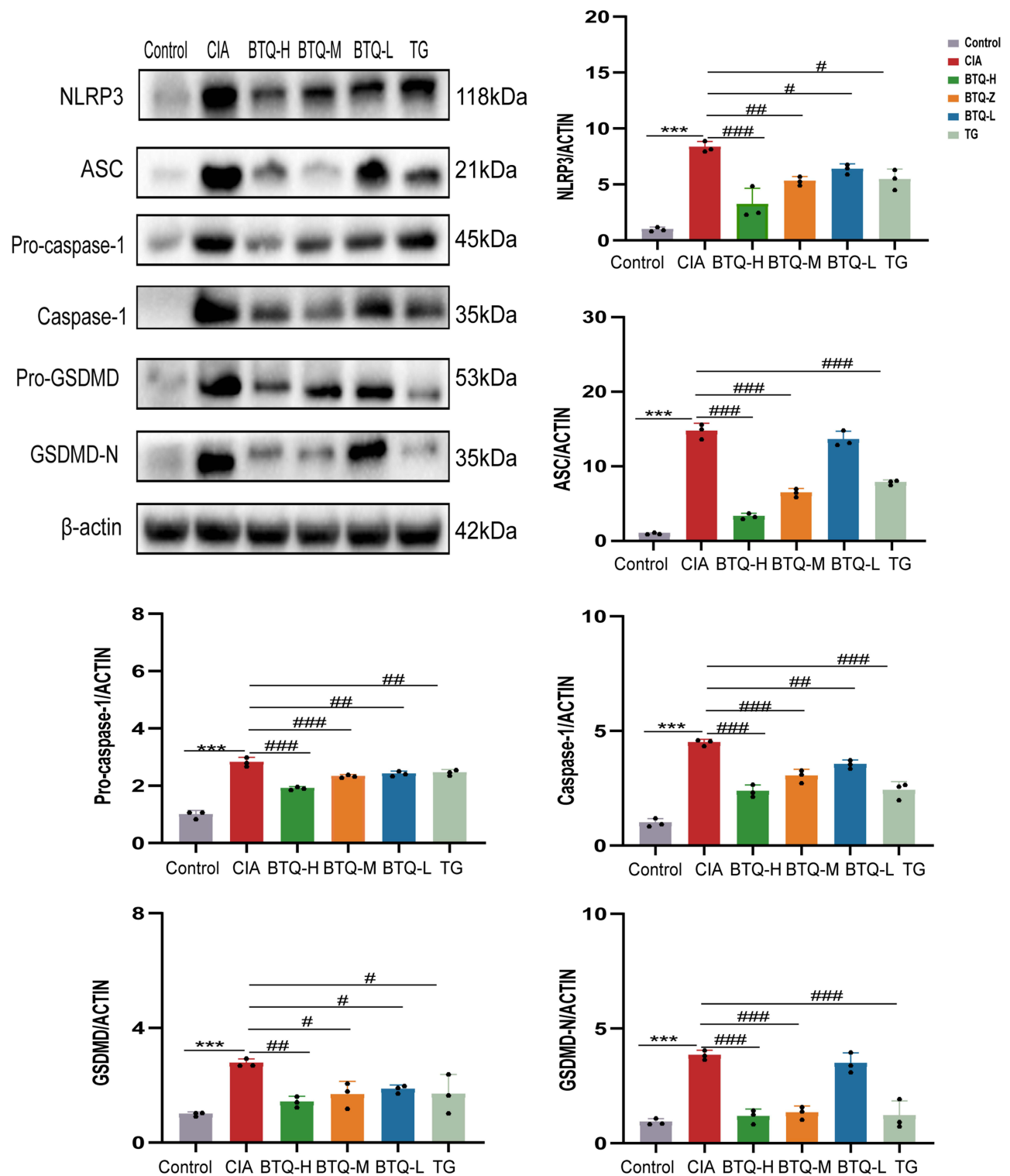


**Figure 5** Western blotting was used to measure the levels of proteins linked to pyroptosis in the synovial tissues of the rats (n=3). \*\*\*,  $p < 0.001$ , respectively, compared with the normal control group; #, ##, and ###,  $p < 0.05$ ,  $p < 0.01$ , and  $p < 0.001$ , respectively, compared with the CIA group.

Immunofluorescence staining revealed an increase in GSDMD expression in Raw264.7 cells stimulated with LPS plus ATP, followed by a notable reduction in GSDMD expression after treatment with BTQ-containing serum (Figure 7A). Similarly, Western blotting experiments showed that treatment with BTQ-containing serum decreased the expression levels of pyroptosis proteins (Figure 7B–G).

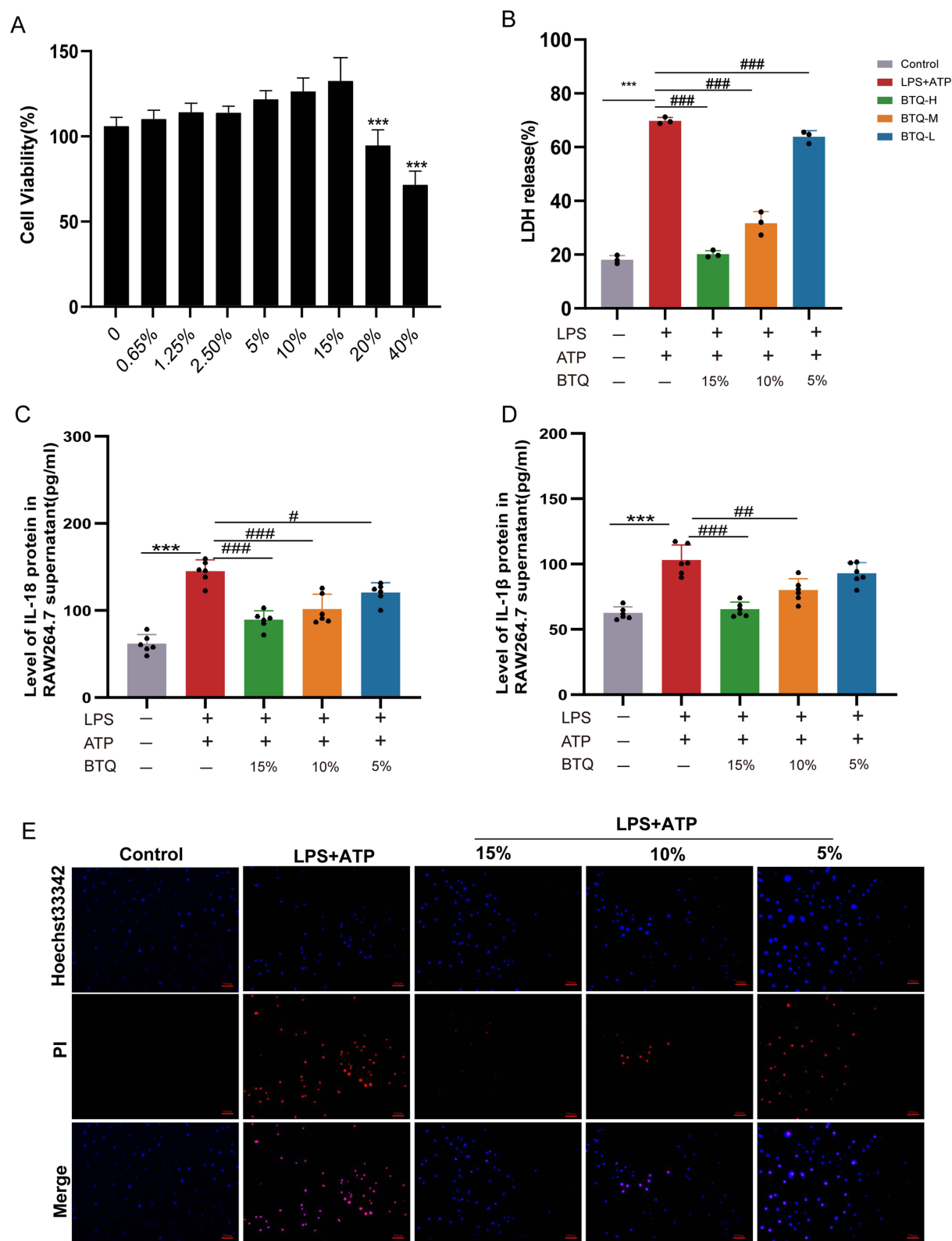


**Figure 6** Inhibitory effect of BTQ on LPS plus ATP induced cell death in Raw264.7 cells. **(A)** CCK8 assay was used to determine the concentrations of BTQ administered. **(B)** LDH release in culture supernatants of RAW264.7 macrophages (n=3). **(C and D)** ELISA was utilized to determine the presence of secreted IL-1 $\beta$  and IL-18 in the culture supernatants of Raw 264.7 cells (n=6). **(E)** PI staining of dead Raw264.7 cells (PI, red; Hoechst 33342, blue. Scale bars = 100  $\mu$ m). \*\*\*,  $p < 0.001$ , respectively, compared with the normal control group; #, ##, and ###,  $p < 0.05$ ,  $p < 0.01$ , and  $p < 0.001$ , respectively, compared with the CIA group.

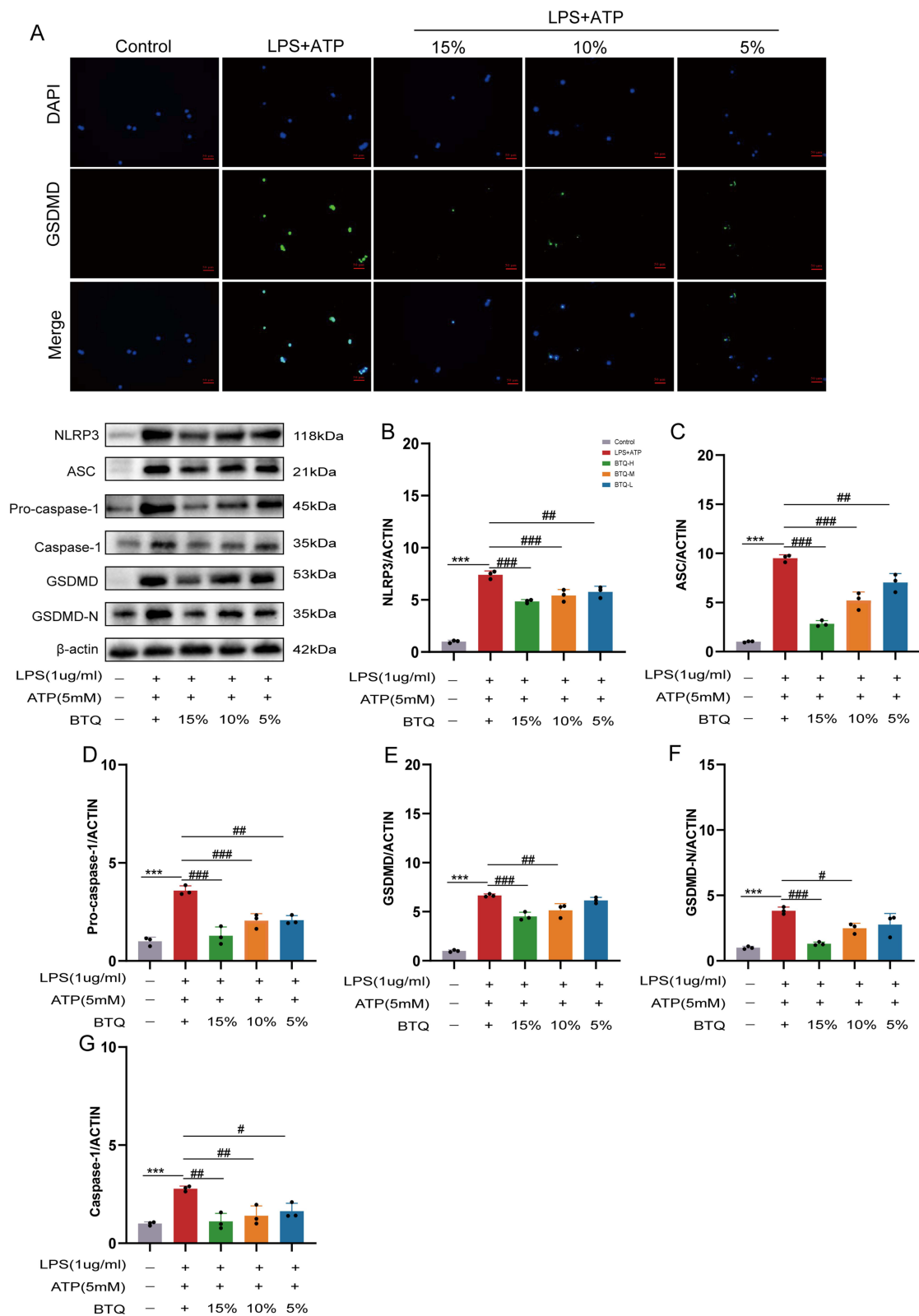


**Figure 7** BTQ inhibits NLRP3 inflammasome induced pyroptosis in Raw264.7 cells. **(A)** GSDMD protein expression (GSDMD FITC green, DAPI blue; scale bar represents 50 $\mu$ m) in Raw264.7 macrophages after LPS plus ATP-induced pyroptosis. **(B–G)** The expression levels of NLRP3, ASC, pro-caspase-1, caspase-1, GSDMD and GSDMD-N in Raw 264.7 cells were detected via Western blotting (n=3). \*\*\*,  $p < 0.001$ , respectively, compared with the normal control group; #, ##, and ###,  $p < 0.05$ ,  $p < 0.01$ , and  $p < 0.001$ , respectively, compared with the CIA group.

## Discussion

In this study, our results show that BTQ can alleviate joint inflammation in CIA rats by inhibiting macrophage pyroptosis, which provides a theoretical basis for the clinical treatment of RA with BTQ. As an autoimmune disease, rheumatoid arthritis affects multiple joints throughout the body. Synovitis is the primary pathological condition, and prolonged synovitis leads to joint damage and deformities that affect patients' daily activities.<sup>33</sup> Due to their pathological similarities to RA, CIA rats serve as a traditional model for research into the development of RA and novel treatment medications.<sup>34,35</sup> Accumulating clinical data indicate that the immune response is dysregulated in RA patients, triggering immune cell activation, with activated macrophages contributing significantly to RA-related inflammation via NLRP3-induced pyroptosis, resulting in prolonged synovitis and cartilage degradation.<sup>8,36</sup> Pyroptosis, a form of programmed cell death, leads to an imbalance of the immune system in patients with RA.<sup>12,15,37,38</sup> Therefore, innovative approaches for the clinical prevention and treatment of RA may emerge from comprehensive research on pyroptosis inhibition, especially macrophage pyroptosis.

GSDMD is the executor of pyroptosis, and its activation implies the onset of pyroptosis.<sup>39,40</sup> The present research revealed increased expression of GSDMD in CIA rats, indicating a greater incidence of pyroptosis in these rats and suggesting the role of pyroptosis in the development of the CIA rats. A multitude of studies indicate that pyroptosis initiation triggers the emission of substantial quantities of inflammatory cytokines, culminating in a localized inflammatory reaction.<sup>41</sup> Research has revealed higher serum concentrations of IL-18 and IL-1 $\beta$  in CIA rats than in control rats. Pyroptosis occurs in CIA rats and leads to the massive production of the cytokines IL-18 and IL-1 $\beta$ , which results in localized inflammation in CIA rats. NLRP3, a key mediator of pyroptosis, is activated by microbial invasion and injury signals, joins forces with ASC and caspase-1 precursors to create the active NLRP3 inflammatory complex, and subsequently liberates mature caspase-1.<sup>42</sup> Caspase-1 subsequently cleaves GSDMD into its N-terminus, leading to the N-terminus of GSDMD engaging with the plasma membrane and triggering pyroptosis.<sup>43</sup> Our current research revealed increased expression of pyroptosis-associated proteins in CIA rats, which is consistent with the above findings. This finding suggested that the unusual activation of the NLRP3/Caspase-1/GSDMD signaling pathway plays a role in the pathological process of pyroptosis observed in CIA rats.

Chinese medicine is a vast treasure trove. It plays a crucial role in the treatment of diseases with complex pathogenesis.<sup>44</sup> Indeed, numerous research works have indicated a link between treating RA with TCM and the alteration of pyroptosis-related pathways. Jinwujiangu capsule (JWJGC) modulates NLRP3/CAPSES/GSDMD pathway to inhibit fibroblast-like Synoviocytes in RA.<sup>45</sup> In addition, Licorice-processed DGN products displayed anti-inflammatory effects via the TLR4/NF- $\kappa$ B/NLRP3 signaling pathway on CIA rats and LPS-induced RAW264.7 cells in treating RA.<sup>46</sup> However, these studies did not explore the relationship between RA treatment with TCM and macrophage pyroptosis. Our current research initially pinpointed the key elements of BTQ using LC-MS. Subsequently, both in vivo and in vitro studies were carried out to investigate the mechanism of action of BTQ in RA treatment. During the experiments conducted in vivo, BTQ was found to inhibit joint inflammation, reduce arthritis scores, tissue swelling, and spleen and thymus indices; and restore body weight in CIA rats. Moreover, BTQ downregulated the expression of NLRP3-mediated pyroptosis-related proteins and inhibited the cytokine levels of IL-18 and IL-1 $\beta$  in the synovium of CIA rats. Considering the impact of BTQ on the expression of crucial proteins involved in pyroptosis, we propose that BTQ might prevent pyroptosis in CIA rats through the control of the NLRP3/Caspase-1/GSDMD pathway. To confirm this hypothesis, RAW264.7 macrophages were subjected to pyroptosis in vitro, and subsequently treated with varying concentrations of BTQ to determine whether BTQ inhibited pyroptosis through the NLRP3/Caspase-1/GSDMD pathway. Macrophages serve as important immune cells in the pathogenesis of RA, and early studies have shown that LPS can activate the NLRP3 inflammasome in macrophages; in addition, macrophages activated with ATP can secrete active IL-1 $\beta$ .<sup>47,48</sup> Thus, RAW264.7 macrophages are stimulated using a combination of LPS and ATP. The detection of crucial proteins within the NLRP3/Caspase-1/GSDMD pathway was performed. These findings indicate that the levels of pyroptosis-associated proteins increase in macrophages stimulated with LPS and ATP. Various concentrations of BTQ were introduced into the macrophage culture medium to monitor the impact of BTQ on crucial proteins in the NLRP3/Caspase-1/GSDMD



pathway, and the findings showed that BTQ can suppress excessive proteins expression. Moreover, BTQ also decreased the LDH, IL-1 $\beta$  and IL-18 levels in macrophages.

The present research revealed that BTQ mitigated joint inflammation in CIA rats through the suppression of NLRP3-induced macrophage pyroptosis, serving as a deep directive for the medical care of RA patients. This research has certain limitations. Firstly, intercellular communication persists among diverse cell types in animal experiments. Future studies should investigate the potential involvement of BTQ in regulating other cellular functions for the treatment of RA. Additionally, it is crucial to employ Multi-omics research methods to elucidate the therapeutic effects of BTQ and provide scientific support for its role in inhibiting NLRP3 inflammasome in RA treatment. Lastly, further research is warranted to explore whether BTQ exerts its therapeutic effects on RA through alternative signaling pathways.

## Conclusions

BTQ effectively mitigates synovial inflammation and cartilage damage in CIA rats. Mechanistic investigations have elucidated the potential therapeutic mechanism of BTQ through inhibition of the NLRP3/Caspase-1/GSDMD pathway in RA.

## Abbreviations

CIA, collagen-induced arthritis; LPS, lipopolysaccharide; NLRP3, NOD-like receptor thermal protein domain-associated protein 3; RA, rheumatoid arthritis; BSA, bovine serum albumin; ATP, adenosine triphosphate; LDH, lactate dehydrogenase; DMARDs, disease-modifying anti-rheumatic drugs; GSDMD, Gasdermin D; IL-1 $\beta$ , interleukin-1 $\beta$ ; IL-18, interleukin-18; NSAIDs, non-steroidal anti-inflammatory drugs; CCK-8, cell counting kit-8; DAPI, 4,6-diamidino-2-phenylindole; PI, Propidium Iodide; PBS, Phosphate Buffered Saline; FBS, fetal bovine serum; PVDF, polyvinylidene difluoride; ASC, apoptosis-associated speck-like protein containing a caspase activation and recruitment domain; SDS-PAGE, sodium dodecyl sulfate-polyacrylamide gel electrophoresis.

## Data Sharing Statement

Every piece of data related to this study can be obtained by making a reasonable request from the corresponding author-Wen Zhu.

## Ethics Statement

This study was approved by the Experimental Animal Ethics Committee of Nanjing University of Chinese Medicine (approval number: 202210A049). All animal studies were performed in accordance with the guidelines and regulations for the use and care of animals at the Centre for Laboratory Animal Care, Nanjing University of Chinese Medicine.

## Acknowledgment

The National Natural Science Foundation of China (Grant number 81973769) provided funding for this research.

## Author Contributions

All authors made a significant contribution to the work reported, whether that is in the conception, study design, execution, acquisition of data, analysis and interpretation, or in all these areas. All authors drafted, revised or reviewed the article, and agreed on the journal in which the article will be submitted, gave final approval for the version to be published. All authors agree to be accountable for all aspects of the work.

## Disclosure

The authors have no conflicts of interest to declare for this work.

## References

1. Smolen JS, Aletaha D, McInnes IB. Rheumatoid arthritis. *Lancet*. 2016;388(10055):2023–2038. doi:10.1016/S0140-6736(16)30173-8
2. Scott DL, Wolfe F, Huizinga TW. Rheumatoid arthritis. *Lancet*. 2010;376(9746):1094–1108. doi:10.1016/S0140-6736(10)60826-4

3. Myasoedova E, Crowson CS, Kremers HM, Thorneau TM, Gabriel SE. Is the incidence of rheumatoid arthritis rising? Results from Olmsted County, Minnesota, 1955–2007. *Arthritis Rheum.* 2010;62(6):1576–1582. doi:10.1002/art.27425
4. Burmester GR, Pope JE. Novel treatment strategies in rheumatoid arthritis. *Lancet.* 2017;389(10086):2338–2348. doi:10.1016/S0140-6736(17)31491-5
5. Prasad P, Verma S, Surbhi, Ganguly NK, Chaturvedi V, Mittal SA. Rheumatoid arthritis: advances in treatment strategies. *Mol Cell Biochem.* 2023;478(1):69–88. doi:10.1007/s11010-022-04492-3
6. Sparks JA. Rheumatoid Arthritis. *Ann Intern Med.* 2019;170(1):1tc1–1tc16. doi:10.7326/AITC201901010
7. Wang Y, Chen SJ, Du KZ, et al. Traditional herbal medicine: therapeutic potential in rheumatoid arthritis. *J Ethnopharmacol.* 2021;279:114368. doi:10.1016/j.jep.2021.114368
8. Edilova MI, Akram A, Abdul-Sater AA. Innate immunity drives pathogenesis of rheumatoid arthritis. *Biomed J.* 2021;44(2):172–182. doi:10.1016/j.bj.2020.06.010
9. Saha S, Shalova IN, Biswas SK. Metabolic regulation of macrophage phenotype and function. *Immunol Rev.* 2017;280(1):102–111. doi:10.1111/imr.12603
10. Siouti E, Andreaskos E. The many facets of macrophages in rheumatoid arthritis. *Biochem Pharmacol.* 2019;165:152–169. doi:10.1016/j.bcp.2019.03.029
11. Yang X, Chang Y, Wei W. Emerging role of targeting macrophages in rheumatoid arthritis: focus on polarization, metabolism and apoptosis. *Cell Prolif.* 2020;53(7):e12854. doi:10.1111/cpr.12854
12. Zhai Z, Yang F, Xu W, et al. Attenuation of Rheumatoid Arthritis Through the Inhibition of Tumor Necrosis Factor-Induced Caspase 3/Gasdermin E-Mediated Pyroptosis. *Arthritis Rheumatol.* 2022;74(3):427–440. doi:10.1002/art.41963
13. Zhao J, Jiang P, Guo S, Schrodi SJ, He D. Apoptosis, Autophagy, NETosis, Necroptosis, and Pyroptosis Mediated Programmed Cell Death as Targets for Innovative Therapy in Rheumatoid Arthritis. *Front Immunol.* 2021;12:809806. doi:10.3389/fimmu.2021.809806
14. You R, He X, Zeng Z, Zhan Y, Xiao Y, Xiao R. Pyroptosis and Its Role in Autoimmune Disease: a Potential Therapeutic Target. *Front Immunol.* 2022;13:841732. doi:10.3389/fimmu.2022.841732
15. Shi J, Gao W, Shao F. Pyroptosis: gasdermin-Mediated Programmed Necrotic Cell Death. *Trends Biochem Sci.* 2017;42(4):245–254. doi:10.1016/j.tibs.2016.10.004
16. Kovacs SB, Miao EA. Gasdermins: effectors of Pyroptosis. *Trends Cell Biol.* 2017;27(9):673–684. doi:10.1016/j.tcb.2017.05.005
17. Jorgensen I, Zhang Y, Krantz BA, Miao EA. Pyroptosis triggers pore-induced intracellular traps (PITs) that capture bacteria and lead to their clearance by efferocytosis. *J Exp Med.* 2016;213(10):2113–2128. doi:10.1084/jem.20151613
18. Huang Y, Jiang H, Chen Y, et al. Tranilast directly targets NLRP3 to treat inflammasome-driven diseases. *EMBO Mol Med.* 2018;10(4). doi:10.15252/emmm.201708689
19. Guo C, Fu R, Wang S, et al. NLRP3 inflammasome activation contributes to the pathogenesis of rheumatoid arthritis. *Clin Exp Immunol.* 2018;194(2):231–243. doi:10.1111/cei.13167
20. Lee HM, Kim JJ, Kim HJ, Shong M, Ku BJ, Jo EK. Upregulated NLRP3 inflammasome activation in patients with type 2 diabetes. *Diabetes.* 2013;62(1):194–204. doi:10.2337/db12-0420
21. Zeng W, Wu D, Sun Y, et al. The selective NLRP3 inhibitor MCC950 hinders atherosclerosis development by attenuating inflammation and pyroptosis in macrophages. *Sci Rep.* 2021;11(1):19305. doi:10.1038/s41598-021-98437-3
22. Wang Y, Zhu W, Lu D, Zhang C, Wang Y. Tetrahydropalmitate attenuates MSU crystal-induced gouty arthritis by inhibiting ROS-mediated NLRP3 inflammasome activation. *Int Immunopharmacol.* 2021;100:108107. doi:10.1016/j.intimp.2021.108107
23. Zhang P, Li J, Han Y, Yu XW, Qin L. Traditional Chinese medicine in the treatment of rheumatoid arthritis: a general review. *Rheumatol Int.* 2010;30(6):713–718. doi:10.1007/s00296-010-1370-0
24. Liu H, Liu S, Wang Y, Xiong Y, Lu L. Serum Metabonomics of Qinjiao Dihuang Tongbi Decoction in the Treatment of Active Rheumatoid Arthritis with Damp-heat Toxin Accumulation Syndrome. *J Tradit Chin Med.* 2022;63:245–250.
25. Chen Y. *Clinical Observation on the Treatment of Rheumatoid Arthritis in Active Stage by Heat-Clearing, Removing Blood Stasis and Detoxification Method and Its Effects on Cytokines.* Nanjing University Chinese Medical; 2019.
26. Li W, Wang K, Liu Y, et al. A Novel Drug Combination of Mangiferin and Cinnamic Acid Alleviates Rheumatoid Arthritis by Inhibiting TLR4/NFκB/NLRP3 Activation-Induced Pyroptosis. *Front Immunol.* 2022;13:912933. doi:10.3389/fimmu.2022.912933
27. National Institutes of Health (US). Laboratory animal welfare: public Health Service policy on humane care and use of laboratory animals by awardee institutions; notice. *Fed Regist.* 1985;50(90):19584–19585.
28. Brand DD, Latham KA, Rosloniec EF. Collagen-induced arthritis. *Nature Protocols.* 2007;2(5):1269–1275. doi:10.1038/nprot.2007.173
29. Deng Y, Luo H, Shu J, et al. Pien Tze Huang alleviate the joint inflammation in collagen-induced arthritis mice. *Chin Med.* 2020;15(1):30. doi:10.1186/s13020-020-00311-3
30. Liu W, Zhang Y, Zhu W, et al. Sinomenine Inhibits the Progression of Rheumatoid Arthritis by Regulating the Secretion of Inflammatory Cytokines and Monocyte/Macrophage Subsets. *Front Immunol.* 2018;9. doi:10.3389/fimmu.2018.02228
31. Liu X, Xia S, Zhang Z, Wu H, Lieberman J. Channelling inflammation: gasdermins in physiology and disease. *Nat Rev Drug Discov.* 2021;20(5):384–405. doi:10.1038/s41573-021-00154-z
32. Yu P, Zhang X, Liu N, Tang L, Peng C, Chen X. Pyroptosis: mechanisms and diseases. *Signal Transduct Target Ther.* 2021;6(1):128. doi:10.1038/s41392-021-00507-5
33. Jang S, Kwon EJ, Lee JJ. Rheumatoid Arthritis: pathogenic Roles of Diverse Immune Cells. *Int J Mol Sci.* 2022;23(2):905. doi:10.3390/ijms23020905
34. Brand DD, Kang AH, Rosloniec EF. Immunopathogenesis of collagen arthritis. *Springer Semin Immunopathol.* 2003;25(1):3–18. doi:10.1007/s00281-003-0127-1
35. Wu J, Feng Z, Chen L, et al. TNF antagonist sensitizes synovial fibroblasts to ferroptotic cell death in collagen-induced arthritis mouse models. *Nat Commun.* 2022;13(1):676. doi:10.1038/s41467-021-27948-4
36. Spel L, Martinon F. Inflammasomes contributing to inflammation in arthritis. *Immunol Rev.* 2020;294(1):48–62. doi:10.1111/imr.12839
37. Choulaki C, Papadaki G, Repa A, et al. Enhanced activity of NLRP3 inflammasome in peripheral blood cells of patients with active rheumatoid arthritis. *Arthritis Res Ther.* 2015;17(1):257. doi:10.1186/s13075-015-0775-2

38. Zhang X, Wang Q, Cao G, Luo M, Hou H, Yue C. Pyroptosis by NLRP3/caspase-1/gasdermin-D pathway in synovial tissues of rheumatoid arthritis patients. *J Cell Mol Med*. 2023;27(16):2448–2456. doi:10.1111/jcmm.17834
39. Ding J, Wang K, Liu W, et al. Pore-forming activity and structural autoinhibition of the gasdermin family. *Nature*. 2016;535(7610):111–116. doi:10.1038/nature18590
40. Burdette BE, Esparza AN, Zhu H, Wang S. Gasdermin D in pyroptosis. *Acta Pharmaceutica Sinica B*. 2021;11(9):2768–2782. doi:10.1016/j.apsb.2021.02.006
41. Coll RC, Schroder K, Pelegrin P. NLRP3 and pyroptosis blockers for treating inflammatory diseases. *Trends Pharmacol Sci*. 2022;43(8):653–668. doi:10.1016/j.tips.2022.04.003
42. Paik S, Kim JK, Silwal P, Sasakawa C, Jo E-K. An update on the regulatory mechanisms of NLRP3 inflammasome activation. *Cell. Mol. Immunol*. 2021;18(5):1141–1160. doi:10.1038/s41423-021-00670-3
43. Xu L, Wang H, Q-q Y, et al. The monomer derivative of paeoniflorin inhibits macrophage pyroptosis via regulating TLR4/ NLRP3/ GSDMD signaling pathway in adjuvant arthritis rats. *Int Immunopharmacol*. 2021;101:108169.
44. Moudgil KD, Berman BM. Traditional Chinese medicine: potential for clinical treatment of rheumatoid arthritis. *Expert Rev Clin Immunol*. 2014;10(7):819–822. doi:10.1586/1744666X.2014.917963
45. Ling Y, Xiao M, Huang Z-W, et al. Jinwujiangu Capsule Treats Fibroblast-Like Synoviocytes of Rheumatoid Arthritis by Inhibiting Pyroptosis via the NLRP3/CAPSES/GSDMD Pathway. *Evid Based Complement Alternat Med*. 2021;2021:1–10.
46. Meng X, Zhang X, Su X, et al. Daphnes Cortex and its licorice-processed products suppress inflammation via the TLR4/NF- $\kappa$ B/NLRP3 signaling pathway and regulation of the metabolic profile in the treatment of rheumatoid arthritis. *J Ethnopharmacol*. 2022;283:114657.
47. Li Z, Jia Y, Feng Y, et al. Methane alleviates sepsis-induced injury by inhibiting pyroptosis and apoptosis: in vivo and in vitro experiments. *Aging*. 2019;11(4):1226–1239. doi:10.18632/aging.101831
48. Demarco B, Danielli S, Fischer FA, Bezradica JS. How Pyroptosis Contributes to Inflammation and Fibroblast-Macrophage Cross-Talk in Rheumatoid Arthritis. *Cells*. 2022;11(8). doi:10.3390/cells11081307

## Journal of Inflammation Research

Dovepress

### Publish your work in this journal

The Journal of Inflammation Research is an international, peer-reviewed open-access journal that welcomes laboratory and clinical findings on the molecular basis, cell biology and pharmacology of inflammation including original research, reviews, symposium reports, hypothesis formation and commentaries on: acute/chronic inflammation; mediators of inflammation; cellular processes; molecular mechanisms; pharmacology and novel anti-inflammatory drugs; clinical conditions involving inflammation. The manuscript management system is completely online and includes a very quick and fair peer-review system. Visit <http://www.dovepress.com/testimonials.php> to read real quotes from published authors.

Submit your manuscript here: <https://www.dovepress.com/journal-of-inflammation-research-journal>